Mon. Not. R. Astron. Soc. **360,** 1143–1152 (2005) doi:10.1111/j.1365-2966.2005.09114.x

Time-dependent convection seismic study of five γ Doradus stars

M.-A. Dupret,[1,2]★ A. Grigahcène,[1,3] R. Garrido,[1] J. De Ridder,[4] R. Scuflaire[5] and M. Gabriel[5]

[1]*Instituto de Astrofísica de Andalucía-CSIC, Apartado 3004, 18080 Granada, Spain*
[2]*Observatoire de Paris, LESIA, 92195 Meudon, France*
[3]*CRAAG – Algiers Observatory BP 63 Bouzareah 16340, Algiers, Algeria*
[4]*Instituut voor Sterrenkunde, Katholieke Universiteit Leuven, Celestijnenlaan 200 B, 3001 Leuven, Belgium*
[5]*Institut d'Astrophysique et de Géophysique de l'Université de Liège, Liège, Belgium*

Accepted 2005 April 11. Received 2005 April 10; in original form 2005 March 21

ABSTRACT

We apply for the first time the time-dependent convection (TDC) treatment of Gabriel and Grigahcène et al. to the photometric mode identification in γ Doradus (γ Dor) stars. We consider the influence of this treatment on the theoretical amplitude ratios and phase differences. Comparison with the observed amplitudes and phases of the stars γ Dor, 9 Aurigae, HD 207223 = HR 8330, HD 12901 and 48501 is presented and enables us to identify the degree ℓ of the pulsation modes for four of them. We also determine the mode stability for different models of these stars. We show that our TDC models agree better with observations than with frozen convection models. Finally, we compare the results obtained with different values of the mixing-length parameter α.

Key words: convection – stars: interiors – stars: oscillations – stars: variables: other.

1 INTRODUCTION

γ Doradus (γ Dor) stars are variable F-type main-sequence stars, whose long periods (from 0.35 to 3 d) correspond to high-order gravity modes (g modes) of pulsation. Many of them are multiperiodic. As g modes probe the deep stellar interiors, γ Dor stars are very good potential targets for asteroseismology. From a theoretical point of view, the driving of their g modes is explained by a flux blocking mechanism at the base of their convective envelope (CE), as shown by Guzik et al. (2000) with frozen convection (FC) models and by Dupret et al. (2004) and Dupret et al. (2005) with time-dependent convection (TDC) models (Gabriel 1996). Theoretical instability strips have been obtained by Warner, Kaye & Guzik (2003), Dupret et al. (2004) and Grigahcène et al. (2004).

However, the mode identification (first step of any seismic study) is particularly difficult for γ Dor stars. The theoretical frequency spectrum corresponding to high-order g modes is very dense, while only a few modes are observed in practice. The mode selection mechanism and the effect of rotation on the frequencies, amplitudes and phases are not known in γ Dor stars (perturbation theories of rotation–pulsation interaction are unrealistic in these long period variables). Mode identification methods based on other observables such as photometric amplitude ratios and line-profile variations are thus required. Concerning the photometry, observing the amplitudes and phases in different passbands makes the identification of the degree ℓ of the modes possible (Balona & Stobie 1979; Watson 1988). Two important theoretical ingredients in this method are the amplitude ($f_{\rm T}$) and phase ($\psi_{\rm T}$) of local effective temperature variation for a normalized radial displacement. Garrido (2000) and Aerts et al. (2004) applied the method to γ Dor stars, considering $f_{\rm T}$ and $\psi_{\rm T}$ as free parameters. These two parameters can be determined by non-adiabatic computations (Dupret et al. 2003b). However, Dupret et al. (2003a) showed that the non-adiabatic theoretical predictions are extremely sensitive to the value adopted for the mixing-length (ML) parameter α and, in all cases, the theoretical amplitude ratios and phase differences obtained with FC models completely disagree with observations.

In this paper, we present for the first time theoretical photometric amplitude ratios and phase differences between the light and velocity curves, as obtained with our TDC models. We apply our models to the mode identification of the stars γ Dor, 9 Aurigae (9 Aur), HD 12901 and 48501. We also compare the theoretical and observed phase differences between the light and velocity curves, for the stars γ Dor, 9 Aur and HD 207223 = HR 8330. These comparisons show that the agreement between theory and observations obtained with our TDC models is much better than with FC models.

2 THEORETICAL MODELS AND NUMERICAL TOOLS

The equilibrium stellar models have been computed by the evolutionary code CLÉS (Code Liégeois d'Évolution Stellaire). It uses the standard mixing length theory (MLT) for convection calculations,

★E-mail: MA.Dupret@obspm.fr

© 2005 RAS

Table 1. Global parameters of the theoretical models adopted for the study of the stars γ Dor, 9 Aur, HD 207223, 12901 and 48501.

	$M/M_\odot$	$T_{\rm eff}$ (K)	$\log(L/L_\odot)$	$\log g$	Z	α
1	1.55	7160.	0.8439	4.1569	0.02	2.0
2	1.55	7160.	0.8394	4.1617	0.02	1.5
3	1.55	7158.	0.8394	4.1610	0.02	1.0
4	1.55	7022.	0.8721	4.0950	0.02	2.0
5	1.55	7015.	0.8684	4.0969	0.02	1.5
6	1.55	7010.	0.8684	4.0958	0.02	1.0
7	1.50	7019.	0.7783	4.1738	0.02	2.0
8	1.50	7012.	0.7645	4.1860	0.02	1.5
9	1.50	7018.	0.7597	4.1922	0.02	1.0
10	1.55	6906.	0.8891	4.0490	0.02	2.00

the OPAL opacities (Iglesias & Rogers 1996) completed at low temperatures with the opacities of Alexander & Ferguson (1994), the CEFF equation of state (Christensen-Dalsgaard & Däppen 1992) and the atmosphere models of Kurucz (1998) as boundary conditions. We give in Table 1 the global parameters of the equilibrium models considered in this study. All these models have $X = 0.7$, $Z = 0.02$ and core overshooting $\alpha_{\rm ov} = 0.2$.

For the non-adiabatic computations, we have used the pulsation code MAD (Dupret 2002). TDC and FC treatments can be adopted in this code. In the TDC case, the perturbation of the convective flux is taken into account, according to Grigahcène et al. (2005). The effect of the full Reynolds stress tensor perturbation will be considered in future works.

3 INFLUENCE OF TIME-DEPENDENT CONVECTION ON NON-ADIABATIC OBSERVABLES

In a linear one-layer approximation and assuming a zero phase for the radial displacement, the theoretical monochromatic magnitude variation of a non-radial mode is given by

$$\begin{aligned}\delta m_\lambda = -\frac{2.5}{\ln 10}\,\epsilon\; & P_\ell^m(\cos i)\, b_{\ell\lambda} \\ & (-(\ell-1)(\ell+2)\,\cos(\sigma t) \\ & +\, f_{\rm T}\,\cos(\sigma t+\psi_{\rm T})\,(\alpha_{{\rm T}\lambda}\,+\,\beta_{{\rm T}\lambda}) \\ & -\, f_g\,\cos(\sigma t)\,(\alpha_{g\lambda}\,+\,\beta_{g\lambda})\,). \end{aligned} \quad (1)$$

The meaning of the different terms and coefficients of this equation is given in Dupret et al. (2003b). The important point here is that some of the coefficients depend on the equilibrium atmosphere model ($b_{\ell\lambda}$, $\alpha_{{\rm T}\lambda}$, $\alpha_{g\lambda}$, $\beta_{{\rm T}\lambda}$, $\beta_{g\lambda}$), while $f_{\rm T}$ and $\psi_{\rm T}$ (defined in Section 1) can only be obtained by non-adiabatic computations. $f_{\rm g}$ is the relative amplitude of effective gravity variation for a normalized radial displacement, $f_{\rm g} \simeq 2 + (\sigma\tau_{\rm dyn})^2 \simeq 2$ for the high-order g modes of γ Dor stars. Linear pulsation models do not give the absolute amplitudes. Theoretical amplitude ratios and phase differences between different photometric passbands can be determined by integrating equation (1) over the passbands and taking the complex ratios. This equation depends directly on the spherical degree ℓ of the modes. Therefore, comparison between the theoretical and observed amplitude ratios and phase differences makes the identification of ℓ possible. Moreover, as $f_{\rm T}$ and $\psi_{\rm T}$ depend on the non-adiabatic pulsation models, constraints on these models can be obtained, a procedure we call non-adiabatic asteroseismology.

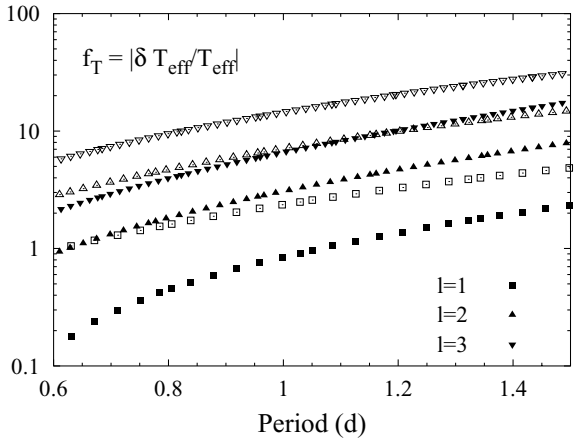

Figure 1. $f_{\rm T}$ as a function of the period (in days), obtained with TDC treatment (full symbols) and FC treatment (empty symbols). Model 4 of Table 1.

Neglecting the effect of non-adiabatic temperature variations on limb darkening, the disc integrated radial velocity of a non-radial mode is given by (Stamford & Watson 1981)

$$V_{\rm r} = \epsilon\sigma R P_\ell^m(\cos i)\left(u_{\ell\lambda} + v_{\ell\lambda}/(\sigma\tau_{\rm dyn})^2\right)\cos(\sigma t - \pi/2), \quad (2)$$

where $u_{\ell\lambda}$ and $v_{\ell\lambda}$ are defined in Stamford & Watson (1981). We see that there is just a $\pi/2$ phase lag between the disc integrated radial velocity and the local radial displacement, so that the phase difference between the light and velocity curves is easily deduced from equation (1).

γ Dor stars have a thin CE whose size increases quickly as $T_{\rm eff}$ decreases. In non-adiabatic models, the coupling between the dynamical and thermal pulsation equations is taken into account. In particular, the perturbation of the radiative and convective flux must be determined in the CE. Usually, the perturbation of convection is neglected, which is the FC approximation. However, this approximation is not justified in a significant part of the CE, because the lifetime of the convective elements is shorter than the pulsation periods. Dupret et al. (2004) and Dupret et al. (2005) showed that the break down of the FC approximation in a significant part of the CE does not greatly affect the interpretation of the driving of the γ Dor stars. This is not the case for the photometric amplitude ratios and the phase differences; we are going to show that the predictions of TDC models are completely different from those of FC models for these observables.

We begin by giving in Figs 1 and 2 the values of $f_{\rm T}$ and $\psi_{\rm T}$ as a function of the period in days, obtained with TDC and FC treatment, for modes of degree $\ell = 1, 2, 3$ and model 4 of Table 1 ($\alpha = 2$). The values of $f_{\rm T}$ are smaller with TDC treatment than with FC treatment. As we are going to show in Section 4, these smaller values of $f_{\rm T}$ in the TDC case imply a better agreement with the typical observed photometric amplitude ratios of γ Dor stars. The values of $\psi_{\rm T}$ are completely different in the TDC and FC cases: they are close to 0° in the TDC case and close to 180° in the FC case. As we are going to show in Section 4, this implies that the phase lags between light and velocity curves predicted by TDC models better agree with the typical observed phase lags in γ Dor stars.

In Figs 3 and 4, we give the real part of $\delta F/F$ as a function of $\log T$, obtained with TDC and FC treatment. This eigenfunction is normalized so that the relative radial displacement is 1 at the photosphere. We compare the results obtained with different values of the ML parameter α. We recall that, at the photosphere,

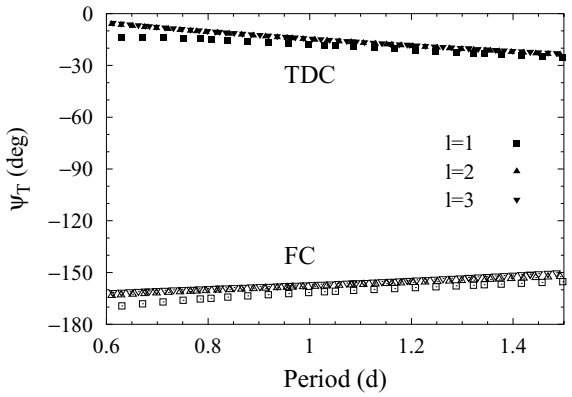

Figure 2. Phase lag ψ_T as a function of the period (in days), obtained with TDC treatment (full symbols) and FC treatment (empty symbols). Model 4 of Table 1.

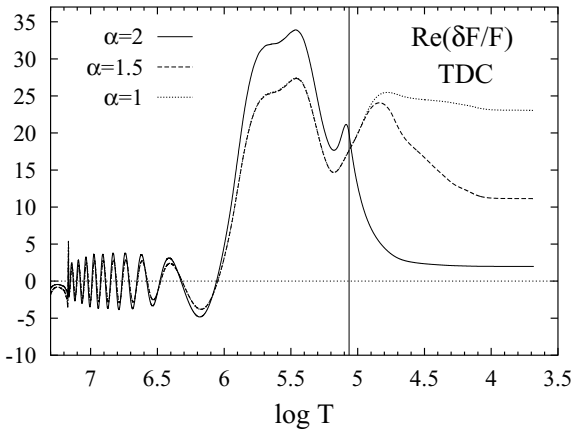

Figure 3. $\Re\{\delta F/F\}$ (relative variation of the radial component of the total flux) as a function of $\log T$, obtained with TDC treatment, for the mode $\ell = 1$, $g_{22}(f = 1.192$ c/d) and models 4–6 of Table 1. The vertical line gives the bottom of the CE, for the $\alpha = 2$ model.

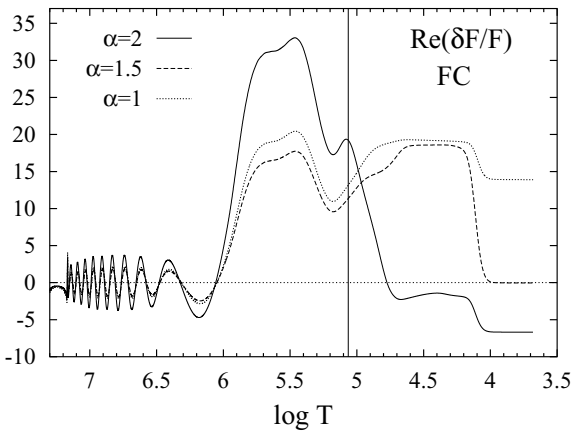

Figure 4. Same caption as Fig. 3 but with FC treatment.

$|\delta F/F| = 4\, f_T$ and $\phi(\delta F/F) = \psi_T$. Comparing the results obtained for $\alpha = 2$ (solid lines) enables us to explain the very different values of f_T and ψ_T obtained in the TDC and FC cases. In both cases, a first decrease of $\Re(\delta F/F)$ occurs in the Fe partial ionization zone ($\log T \simeq 5.3$), it is owing to a κ mechanism similar to the case of slowly pulsating B stars. A second decrease of $\Re(\delta F/F)$ occurs near the base of the CE ($\log T \simeq 5$). This corresponds to the flux blocking mechanism described in details by Guzik et al. (2000), Dupret et al. (2004) and Dupret et al. (2005). In the FC case, κ mechanism occurs inside the CE, in the partial ionization zones of HeII ($\log T \simeq 4.8$) and H ($\log T \simeq 4.1$). These κ mechanisms imply additional decreases of $\Re(\delta F/F)$ down to negative values, which explains the phase lags around 180° predicted by the FC models with high α. In contrast, these κ mechanisms inside the CE are not allowed by TDC models, because they would lead to too high superadiabatic gradients. Therefore, $\delta F/F$ remains flat and positive after the flux blocking drop and its phase remains near 0°. For smaller α, the CE base is closer to the surface, so that the flux blocking is less efficient and the drop of $\Re(\delta F/F)$ is smaller; hence, larger values of f_T are predicted and the change of sign of $\Re(\delta F/F)$ no longer occurs in the FC case (for small α).

4 APPLICATIONS

We consider now the applications to several specific γ Dor stars. The main goal of this paper is to compare the predictions of our non-adiabatic calculations with the observed amplitude ratios and phase differences. We have shown in the previous section that the main difference between FC and TDC results is in the theoretical phase lag between the light and velocity curves. Therefore, we chose to study the γ Dor stars for which the most precise multicolour photometric amplitudes and phases are available and/or for which simultaneous spectroscopic and photometric observations were performed.

The methodology of our study is the following. For each star, we select a family of models inside the observational error box for the global parameters $T_{\rm eff}$, $\log g$ and $\log(L/L_\odot)$. For each model, we perform non-adiabatic computations with TDC and FC treatment, we select the modes of different degrees ℓ with theoretical frequencies closest to the observed ones, and compute the non-adiabatic quantities f_T and ψ_T. Then, the integration of equation (1) on the passbands enables us to determine the theoretical photometric amplitude ratios between different photometric passbands and the theoretical phase lags between the light and velocity curves. The phase differences between different photometric passbands are all close to zero and smaller than the associated errors in present ground-based observations of γ Dor stars, in contrast with the case of δ Sct stars for which significant phase differences are observed. Hence, these phase differences do not give relevant information for the photometric mode identification in γ Dor stars and we do not consider them in our study. Finally, the comparison with the observations enables us to identify the degrees ℓ of the modes and to see which models best agree with observations. For the determination of the monochromatic flux derivatives and limb-darkening coefficients required in equation (1), two different families of atmosphere models have been considered. On one hand, we use the atmosphere models of Kurucz (1993) and the limb-darkening coefficients of Claret (2000), in which the ML treatment of convection ($\alpha = 1.25$) is adopted, we refer to them as MLT atmosphere models. On the other hand, we use the new atmosphere models of Heiter et al. (2002) and the limb-darkening coefficients of Barban et al. (2003), in which the convection treatment of Canuto, Goldman & Mazzitelli (1996) is adopted, we refer to them as full spectrum of turbulence (FST) atmosphere models. We remark that MLT is always adopted in our interior models, while MLT or FST are used for the atmosphere models. Consistent models with FST treatment in both interior and atmosphere models will be considered in a future paper by Montalban et al.

Table 2. Observed global parameters of γ Dor. Strömgren indices-based calibrations are taken from: Smalley & Kupka (1997)[a], Smalley (1993)[c] and using the Vienna TEMPLOGG v. 2 software (Stütz & Nendwich 2002)[b]. The luminosity (deduced from the *Hipparcos* parallax) and $v \sin i$ are taken from Kaye et al. (1999a)[d].

$T_{\rm eff}$ (K)	$\log(L/L_\odot)$	$\log g$	[M/H]	$v \sin i$ (km s^{-1})
7120[a]	0.845[d]	4.25[a]	−0.02[c]	62[d]
7202[b]		4.23[b]	−0.01[b]	

4.1 γ Doradus

γ Dor (HD 27290) is the prototype and brightest member of the class. In this study, we use the observations by Balona et al. (1994a) and Balona, Krisciunas & Cousins (1994b), who obtained very precise Strömgren photometric amplitudes and phases and the observations by Balona et al. (1996), who observed γ Dor simultaneously in photometry and spectroscopy. From these observations, three modes with frequencies $f_1 = 1.32098$ c/d, $f_2 = 1.36354$ c/d and $f_3 = 1.47447$ c/d are detected. Spectroscopic mode identification by the method of moments was performed by Balona et al. (1996) who found as best solution: $(\ell_1, m_1) = (3, 3)$, $(\ell_2, m_2) = (1, 1)$ and $(\ell_3, m_3) = (1, 1)$. We give in Table 2 the observed global parameters of γ Dor. In the lines 1–3 of Table 1, we give the global characteristics of the theoretical models we have adopted for this star.

4.1.1 Mode stability

Our non-adiabatic pulsation code makes the determination of mode stability possible. For model 1 of Table 1 ($\alpha = 2$), the modes of degree $\ell = 1$–4 with theoretical frequencies closest to the observed ones are all predicted to be unstable. For models 2 and 3 of Table 1 ($\alpha \leqslant 1.5$), the three modes of γ Dor are predicted to be stable. Therefore, from the point of view of mode stability, the models with $\alpha \leqslant 1.5$ must be rejected.

4.1.2 Photometric amplitude ratios

In Fig. 5, we give the theoretical and observed Strömgren photometric amplitude ratios we obtained for different models of γ Dor. The lines are the theoretical predictions for different ℓ and the error bars represent the observations for the f_1 and f_2 frequencies. The photometric amplitudes of f_3 are too small and have large associated errors, therefore we do not consider them in this study. The top panels give the results obtained with TDC treatment and the bottom panels give the results obtained with the FC treatment. The left and middle panels give the results obtained for model 1 and the right panels give the results obtained for model 3 of Table 1. For the left panels FST atmosphere models have been considered, while MLT atmosphere models have been considered for the middle and right panels.

The comparison between theory and observations shows that, from the point of view of the photometric amplitude ratios, the f_1 and f_2 frequencies are identified as $\ell = 1$ modes. The best agreement is found for a model with $\alpha = 2$, FST atmosphere and TDC treatment (top left panel). For all the models, good agreement between the theoretical and observed b/v and y/v amplitude ratios is obtained. The theoretical u/v amplitude ratio is very sensitive to the value of $f_{\rm T}$ and to the adopted atmosphere model. Small values of $f_{\rm T}$ (around 0.5) and FST atmospheres are required to obtain the best agreement with the observed u/v amplitude ratio. We give in the right column of Table 3, the values of $f_{\rm T}$ obtained for models 1, 2 and 3 of Table 1, with TDC and FC treatment. We see that the required small value of $f_{\rm T}$ can only be obtained by TDC models with $\alpha = 2$. Finally, we emphasize that for this best model with small $f_{\rm T}$, the differences between the amplitude ratios corresponding to different ℓ is larger, and only the $\ell = 1$ solution agrees with observations.

Our photometric mode identification agrees with the spectroscopic mode identification of Balona et al. (1996) for component f_2, but they disagree for component f_1. The theoretical photometric amplitude ratios corresponding to $\ell = 1$ and $\ell = 3$ are always predicted to be very different, for any values of $f_{\rm T}$; and the observations indicate that f_1 and f_2 have similar amplitude ratios. Also, more cancellation effects owing to surface integration are expected for

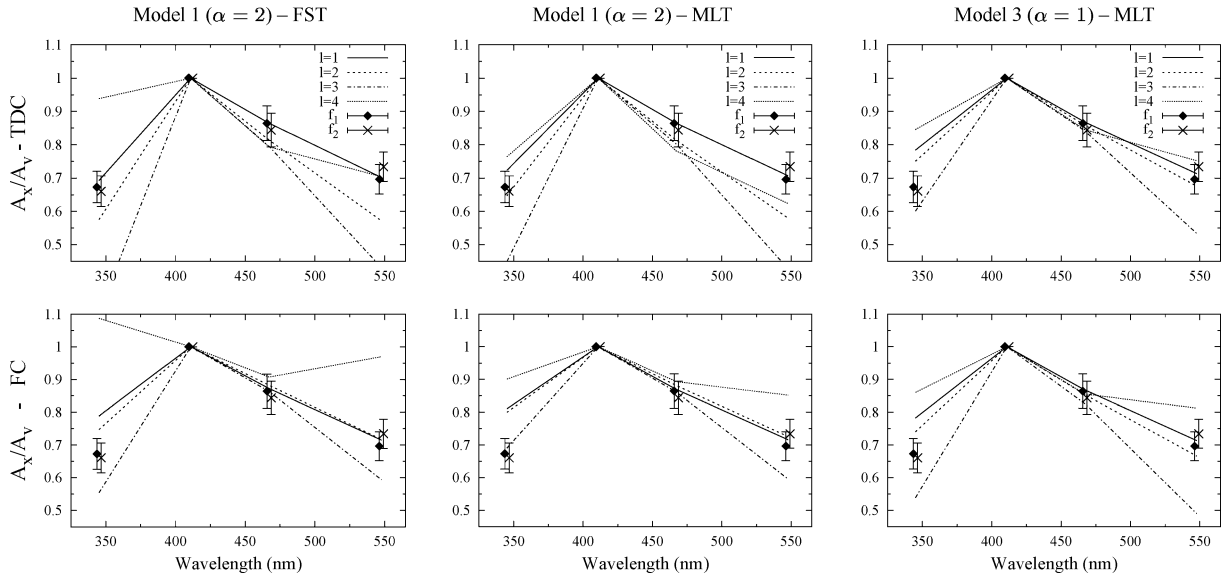

Figure 5. Strömgren photometric amplitude ratios for different models of γ Dor. The top panels are for TDC models and the bottom panels are for FC models. The lines are the theoretical predictions for different ℓ and the error bars represent the observations for the f_1 and f_2 frequencies.

Table 3. Observed phase differences ($\Delta\phi_{\rm obs}$, in degrees) and theoretical phase differences ($\Delta\phi_{\rm th}$) between the photometric flux variations in the Johnson V passband and the radial displacement (radial velocity phase -90°) for the f_2 and f_3 frequencies of γ Dor. The observed phases are taken from Balona et al. (1996). In the right column, we give the theoretical values of $f_{\rm T}$.

Model	conv.	$\ell=1$	$\ell=2$ $\Delta\phi_{\rm th}$	$\ell=3$	$\ell=1$ $f_{\rm T}$
		g_{19}	g_{33}	g_{47}	g_{19}
$f_2=1.364$ c/d		$\Delta\phi_{\rm obs}=-65\pm5$			
1	TDC	−28	−43	−54	0.48
2	TDC	−33	−25	−20	5.28
3	TDC	−18	−15	−12	6.17
1	FC	−167	−166	−167	1.38
2	FC	−61	−74	−143	3.41
3	FC	−28	−25	−34	4.86
		g_{17}	g_{31}	g_{43}	g_{17}
$f_3=1.474$ c/d		$\Delta\phi_{\rm obs}=-29\pm8$			
1	TDC	−27	−48	−74	0.34
2	TDC	−37	−28	−24	4.42
3	TDC	−21	−17	−14	5.16
1	FC	−165	−164	−165	1.21
2	FC	−68	−73	−129	3.13
3	FC	−32	−28	−34	4.23

$\ell=3$ modes. This makes us more confident with our photometric mode identification. Further investigations are required to understand the difference between the spectroscopic and photometric mode identifications for component f_1.

4.1.3 Phase lag between light and velocity curves

Balona et al. (1996) observed γ Dor simultaneously in photometry and spectroscopy and they determined the phase difference between the magnitude variation in Johnson V and the radial velocity variations for each mode. Adding 90° to these phase lags gives the observed phase differences between the observed flux variations in the V band and the local radial displacement ($\Delta\phi_{\rm obs}$). Balona et al. (1996) showed that the radial velocity amplitude of the component f_1 is very small (contrary to its light amplitude) and the error bars are too large. Therefore, we do not consider this mode here. The theoretical phase difference between the flux variation and the local radial displacement ($\Delta\phi_{\rm th}$) is directly obtained by integrating equation (1) on the V band. We give in Table 3 the comparison between the theoretical and observed phase lags for components f_2 and f_3, as obtained for models 1, 2 and 3 of Table 1, with TDC and FC treatment. The phase lags predicted by FC models with $\alpha=2$ completely disagree with the observations. In contrast, theoretical and observational data agree better for all TDC models and for FC models with $\alpha\leqslant1.5$. We recall that the modes are predicted to be stable for the models with $\alpha\leqslant1.5$. Only the TDC models with $\alpha=2$ agree reasonably well with the photometric and spectroscopic observables and predict at the same time the instability of the observed modes. We remark that no significant phase differences between photometric magnitude variations in different passbands are observed for γ Dor. Taking this into account, the value $\Delta\phi_{\rm obs}=-65^\circ$ seems a bit large and must be considered with care, the real phase lag could be closer to 0°.

Table 4. Observed global parameters of 9 Aur. Strömgren indices-based calibrations are taken from: Smalley & Kupka (1997)[a], Smalley (1993)[c] and using the Vienna TEMPLOGG v. 2 software (Stütz & Nendwich 2002)[b]. The luminosity (deduced from the *Hipparcos* parallax) and $v\sin i$ are taken from Kaye et al. (1999a)[d].

$T_{\rm eff}$ (K)	$\log(L/L_\odot)$	$\log g$	[M/H]	$v\sin i$ (km s^{-1})
6990[a]	0.778[d]	4.17[a]	−0.18[c]	18[d]
7050[b]		4.2[b]	−0.20[b]	

4.2 9 Aurigae

9 Aur (HD 32537) is a well known γ Dor type star. In this study, we use the observations by Zerbi et al. (1997), who obtained very precise Strömgren photometric amplitudes and phases in the frame of a multilongitude campaign; we use also the photometric and spectroscopic observations by Krisciunas et al. (1995). Three frequencies $f_1=0.7948$ c/d, $f_2=0.7679$ c/d and $f_3=0.3429$ c/d were detected in the Zerbi et al. campaign. Spectroscopic mode identification by the method of moments was performed by Aerts & Krisciunas (1996), for components f_1 and f_3. They found as the best solution: $(\ell,|m|)=(3,1)$ for both. We give in Table 4 the observed global parameters of 9 Aur. In lines 7–9 of Table 1 we give the global characteristics of the theoretical models we have adopted for this star.

4.2.1 Mode stability

We studied the stability of the modes for different models of 9 Aur. For all the models in the observational error box for $T_{\rm eff}$, $\log L$ and $\log g$, the component with the longest period (f_3) is predicted to be stable. Models with higher luminosity, lower gravity and lower effective temperature are required to obtain the instability of this mode, but these values are out of the observational error box. The components f_1 and f_2 are predicted to be unstable for model 7 of Table 1 ($\alpha=2$) and modes of degree $\ell=1$ and 2. For models 8 and 9 of Table 1 ($\alpha\leqslant1.5$), all the observed modes are predicted to be stable. Therefore, from the point of view of mode stability, the models with $\alpha\leqslant1.5$ must be rejected. The driving of the f_3 component is not explained by models inside the observational ($T_{\rm eff}$, $\log L$, $\log g$) error box; the reasons for this will be investigated in future works.

4.2.2 Photometric amplitude ratios

In Fig. 6, we give the theoretical and observed Strömgren photometric amplitude ratios we obtained for different models of 9 Aur. The left and middle panels give the results obtained for model 7 and the right panels give the results obtained for model 9 of Table 1. For the left panels FST atmosphere models have been considered, while MLT atmosphere models have been considered for the middle and right panels.

The comparison between theory and observations shows that, from the point of view of the photometric amplitude ratios, the three components f_1, f_2 and f_3 are identified most probably as $\ell=2$ modes, but the $\ell=1$ solution cannot be completely eliminated. The best agreement is found for a model with $\alpha=2$, FST atmosphere and TDC treatment (top left). For all the models, good agreement between the theoretical and observed b/v and y/v amplitude ratios is

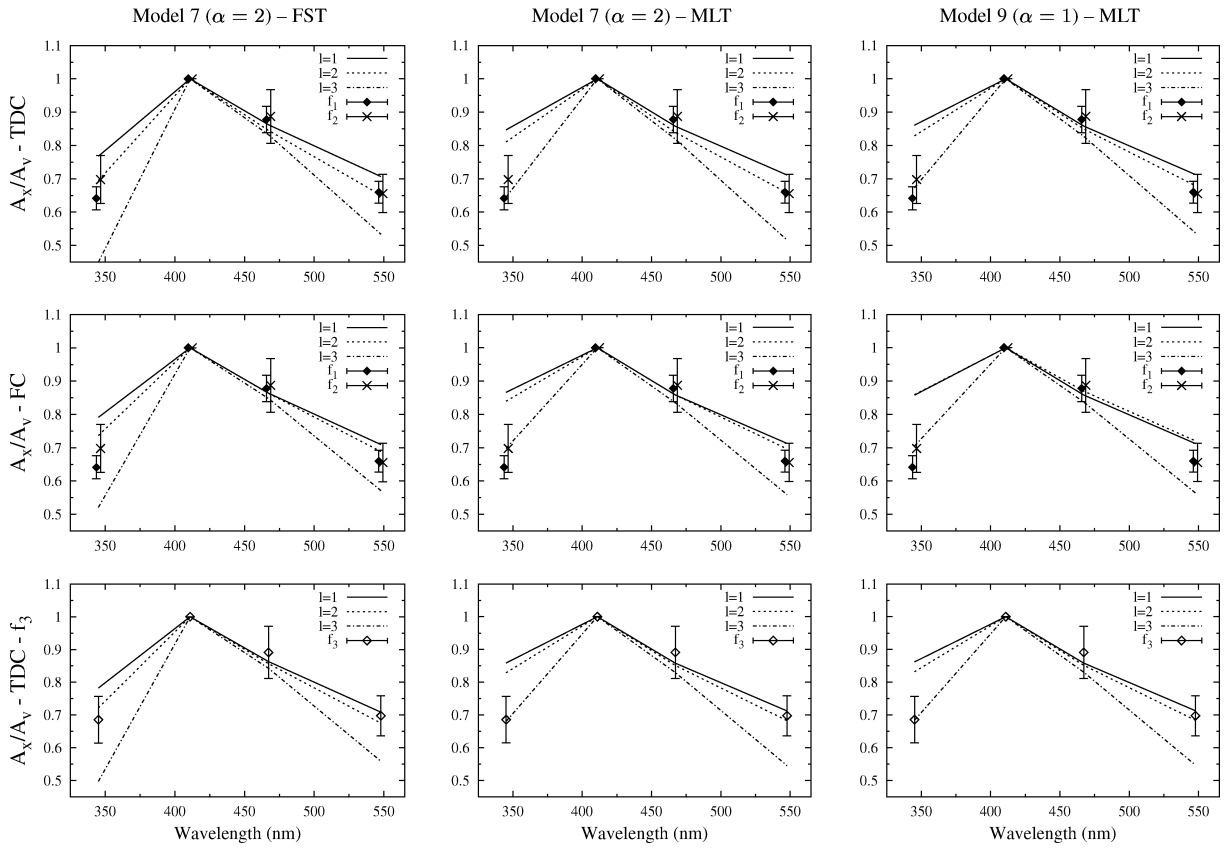

Figure 6. Strömgren photometric amplitude ratios for different models of 9 Aur. The top and middle panels are for modes f_1 and f_2 and the bottom panels are for mode f_3. The top and bottom panels are for TDC models and the middle panels are for FC models. The lines are the theoretical predictions for different ℓ values and the error bars represent the observations for the different frequencies.

obtained. The theoretical u/v amplitude ratio is very sensitive to the value of $f_{\rm T}$ and to the adopted atmosphere model. FST atmospheres are required to obtain the best agreement with the observed u/v amplitude ratio.

The results of our photometric mode identification differ from those of the spectroscopic mode identification by Aerts & Krisciunas (1996), who found $(\ell, |m|) = (3, 1)$ as the best solution for f_1 and f_3. We notice, however, that $\ell = 2$ solutions cannot be eliminated by the line-profile analysis, as shown in table 1 of Aerts & Krisciunas (1996). Further investigations are required to understand the difference between spectroscopic and photometric mode identifications.

4.2.3 Phase lag between light and velocity curves

Zerbi et al. (1997) and Krisciunas et al. (1995) observed 9 Aur simultaneously in photometry and spectroscopy. No radial velocity variations corresponding to f_1 are detected in the observations of Krisciunas et al. (1995) and they have too small an amplitude in the observations of Zerbi et al. (1997); the component f_2 was not detected by Krisciunas et al. (1995). For the other observed components, phase differences between the light and velocity curves could be obtained. In Table 5, we give the theoretical ($\Delta\phi_{\rm th}$) and observed ($\Delta\phi_{\rm obs}$) phase differences between the flux variations in the V band and the local radial displacement, for components f_2 and f_3. No significant phase differences between the photometric magnitude variations in different passbands are observed for 9 Aur. Taking this into account, the value $\Delta\phi_{\rm obs} = -77^\circ$ seems a bit large and must be considered with care, the real phase lag could be closer to 0°. Theoretical results are given for models 7, 8 and 9 of Table 1, with TDC and FC treatment. Observations indicate phase lags between -90°

Table 5. Observed phase differences ($\Delta\phi_{\rm obs}$, in degrees) and theoretical phase differences ($\Delta\phi_{\rm th}$) between the photometric flux variations in the Johnson V passband and the radial displacement for the f_2 and f_3 frequencies of 9 Aur. Observed phases are taken from Zerbi et al. (1997)[a] and Krisciunas et al. (1995)[b]. In the right column, we give the theoretical values of $f_{\rm T}$.

Model	Conv.	$\ell = 1$	$\ell = 2$ $\Delta\phi_{\rm th}$	$\ell = 3$	$\ell = 2$ $f_{\rm T}$
		g_{35}	g_{61}	g_{86}	g_{61}
$f_2 = 0.768$ c/d		$\Delta\phi_{\rm obs} = -77 \pm 12^a$			
7	TDC	−21	−22	−23	8.0
8	TDC	−41	−27	−24	16.0
9	TDC	−11	−10	−11	33.6
7	FC	−157	−156	−156	14.9
8	FC	−110	−164	−172	11.6
9	FC	−22	−157	−175	5.0
		g_{78}	g_{137}	g_{195}	g_{137}
$f_3 = 0.343$ c/d		$\Delta\phi_{\rm obs} = -50 \pm 21^a, -33 \pm 10^b$			
7	TDC	−42	−39	−36	72.4
8	TDC	−40	−38	−36	91.5
9	TDC	−22	−30	−36	112.0
7	FC	−146	−140	−137	88.6
8	FC	−175	−178	−180	111.4
9	FC	−175	−178	−180	126.8

Table 6. Observed global parameters of HD 207223 taken from Aerts & Kaye (2001)[a] (based on Kaye & Gray, in preparation), Kaye et al. (1999b)[c], Kaye et al. (1999a)[d] and using the Vienna TEMPLOGG v. 2 software (Stütz & Nendwich 2002)[b].

$T_{\rm eff}$ (K)	$\log(L/L_\odot)$	$\log g$	[M/H]	$v \sin i$ (km s^{-1})
6985[a]	0.84[c]	4.12[a]	0.08[a]	9.1[c]
6893[b]	0.87[d]	3.96[b]	−0.01[b]	38[d]

and -20°, in reasonably good agreement with the predictions of our TDC models. In contrast, all FC phases (except one) are around 180° and disagree with the observations. Only one FC model has a phase close to 0° (model 9, f_2, $\ell = 1$), but with a small α (= 1) for which the observed modes are predicted to be stable.

4.3 HD 207223 = HR 8330

HD 207223 has been observed simultaneously in *BV* photometry and in high-resolution high signal-to-noise ratio spectroscopy by Kaye et al. (1999b). From these observations, they detected a single frequency $f = 0.3855$ c/d and they could determine the phase lag between the light curve and the radial displacement. Spectroscopic observations and mode identification were performed by Aerts & Kaye (2001) who found as the best solution: $(\ell, m) = (2, 2)$. We give in Table 6 the observed global parameters of HD 207223. In lines 4, 5, 6 and 10 of Table 1 we give the global characteristics of the theoretical models we have adopted for this star.

4.3.1 Mode stability

We studied the stability of the observed mode of HD 207223, for models 4, 5, 6 and 10 of Table 1. For models 4 and 10 ($\alpha = 2$), the mode of degree $\ell = 1$ with frequency closest to the observed one is predicted to be unstable (modes with $\ell \geqslant 2$ are predicted to be stable). For models 5 and 6 ($\alpha \leqslant 1.5$), the mode is predicted to be stable (for any ℓ). Therefore, from the point of view of mode stability, models with $\alpha \leqslant 1.5$ must be rejected.

4.3.2 Phase lag between light and velocity curves

In Table 7, we give the theoretical ($\Delta\phi_{\rm th}$) and observed ($\Delta\phi_{\rm obs}$) phase differences between the flux variations in the *V* band and the local radial displacement. Theoretical results obtained with TDC and FC treatment are given for models 4, 5, 6 and 10 of Table 1, for modes of different ℓ with the theoretical frequency closest to the one observed. Relatively good agreement between theoretical and observational data is obtained for all TDC models. In contrast, all FC phases are around 180° and disagree with the observations.

4.4 HD 12901

HD 12901 was first reported as intrinsically variable by Eyer & Aerts (2000). Extensive Geneva photometry and high-resolution spectroscopy was performed by Aerts et al. (2004) who detected three frequencies: $f_1 = 1.21563$ c/d; $f_2 = 1.39594$ c/d; and $f_3 = 2.18636$ c/d. We give in Table 8 the observed global parameters of HD 12901. In the lines 4–9 of Table 1 we give the global characteristics of the theoretical models we have adopted for this star.

Table 7. Observed phase differences ($\Delta\phi_{\rm obs}$, in degrees) and theoretical phase differences ($\Delta\phi_{\rm th}$) between the photometric flux variations in the Johnson *V* passband and the radial displacement for the star HD 207223. Observed phases are taken from Kaye et al. (1999b).

Model	conv.	$\ell = 1$	$\ell = 2$ $\Delta\phi_{\rm th}$	$\ell = 3$
		g_{69}	g_{119}	g_{171}
$f = 0.38551$ c/d		$\Delta\phi_{\rm obs} = -57 \pm 7$		
4	TDC	−41	−37	−32
5	TDC	−29	−32	−32
6	TDC	−12	−19	−23
10	TDC	−33	−32	−31
4	FC	−149	−159	−170
5	FC	−172	−178	−178
6	FC	−157	−177	−178
10	FC	−153	−151	−150

Table 8. Observed global parameters of HD 12901 obtained using the Vienna TEMPLOGG v. 2 software (Stütz & Nendwich 2002) and Hβ measures by Handler (1999)[a], from Geneva calibrations (Künzli et al. 1997)[b], Aerts et al. (2004)[c] and Mathias et al. (2004)[d].

$T_{\rm eff}$ (K)	$\log g$	[M/H]	$v \sin i$ (km s^{-1})
7014[a]	4.06[a]	−0.38[a]	53[c]
7080[b]	4.47[b]	−0.4[b]	66[d]

4.4.1 Mode stability

We studied the stability of the observed modes of HD 12901 for models 4–9 of Table 1 and for modes with $\ell \leqslant 4$. For models 4 and 7 ($\alpha = 2$), components f_1 and f_2 are always predicted to be unstable; component f_3 is unstable for $\ell \geqslant 2$ and stable for $\ell = 1$. For the other models ($\alpha \leqslant 1.5$), all the observed modes are predicted to be stable. There is only one exception for model 8, in which components f_1, $\ell = 1$ and f_3, $\ell = 2$ are predicted to be unstable (other modes are stable). Therefore, from the point of view of mode stability, models with $\alpha \leqslant 1.5$ must be rejected.

4.4.2 Photometric amplitude ratios

Aerts et al. (2004) showed that $f_{\rm T} \simeq 0.05$ is required to get good agreement between the theoretical and observed amplitude ratios in all passbands, for the star HD 12901; and for this small value of $f_{\rm T}$, the three observed modes are identified as $\ell = 1$ modes. They also showed that with FC treatment it is impossible to get good agreement with observations, because the predicted values of $f_{\rm T}$ are too large.

In Table 9, we give the values of $f_{\rm T}$ and $\psi_{\rm T}$ obtained for models 4–9 of HD 12901, $\ell = 1$ modes and TDC treatment. In agreement with Figs 1 and 3, we see that $f_{\rm T}$ decreases for increasing frequencies (in the domain of the g modes) and increasing α. In Fig. 7, we give the theoretical and observed Geneva photometric amplitude ratios we obtained for different TDC models of HD 12901. Top panels give the results obtained for components f_1 and f_2 and bottom panels for component f_3. The left, middle and right panels give the results obtained for models 4, 7 and 8 of Table 1, respectively. We used MLT atmosphere models in all our computations.

Table 9. Values of f_T and ψ_T (in degrees) obtained for different TDC models of HD 12901, for $\ell = 1$ modes with frequencies closest to the three observed ones.

Model	f_T			ψ_T		
	f_1	f_2	f_3	f_1	f_2	f_3
4	0.52	0.30	0.02	−15	−14	−153
5	3.93	2.65	0.44	−50	−59	−111
6	5.88	4.17	0.77	−23	−28	−71
7	0.71	0.54	0.04	−14	−13	−28
8	2.20	1.47	0.25	−57	−61	−88
9	8.19	6.34	1.68	−21	−25	−53

With TDC treatment and $\alpha = 2$ (left and middle panels of Fig. 7), the values of f_T are the smallest and consequently, a better agreement with observations can be obtained. However, for components f_1 and f_2, the values predicted for f_T are not small enough to give good agreement for the critical U/B_1 amplitude ratio (top panels). For component f_3, f_T is much smaller and good agreement is obtained for model 7 (bottom middle panel). Not only are small f_T values required, but also ψ_T close to 0° is necessary. This explains why the theoretical amplitude ratios of model 4 are unrealistic for f_3 (bottom left panel).

No abundance determination was performed for HD 12901 and, as a first step, we used models with $Z = 0.02$ in the present study. Photometric calibrations indicate that this star could be less metallic than the Sun. In a future study, we will also consider interior and atmospheric models with lower metallicity. Seismic modelling of HD 12901, using a new method based on frequency ratios has been recently performed by Moya et al. (2005). Our future project is to combine TDC and frequencies analysis, for a more complete seismic study of this star.

4.5 HD 48501

HD 48501 was first reported as being intrinsically variable by Eyer & Aerts (2000). Extensive Geneva photometry and high-resolution spectroscopy was performed by Aerts et al. (2004) who detected three frequencies: $f_1 = 1.09408$ c/d, $f_2 = 1.29054$ c/d and $f_3 = 1.19924$ c/d.

Table 10. Observed global parameters of HD 48501 obtained using the Vienna TEMPLOGG v. 2 software (Stütz & Nendwich 2002)[a], from Geneva calibrations (Künzli et al. 1997)[b] and Aerts et al. (2004)[c].

$T_{\rm eff}$ (K)	$\log g$	[M/H]	$v \sin i$ (km s^{-1})
6984[a]	3.92[a]	−0.12[a]	29[c]
7080[b]	4.49[b]	−0.1[b]	

We give in Table 10 the observed global parameters of HD 48501. In lines 4–9 of Table 1 we give the global characteristics of the theoretical models we have adopted for this star.

4.5.1 Mode stability

We studied the stability of the observed modes of HD 48501 for models 4–9 of Table 1 and for modes with $\ell \leqslant 4$. For models 4 and 7 ($\alpha = 2$), the three components are predicted to be unstable for $\ell \leqslant 3$, the modes $\ell = 4$ are unstable for model 4 and component f_3 of model 7. For model 8 ($\alpha = 1.5$), the $\ell = 1$ modes are predicted to be unstable (other modes are stable). For all the other models, all the observed modes are predicted to be stable.

4.5.2 Photometric amplitude ratios

Aerts et al. (2004) showed that a very small $f_T \simeq 0.1$ is required to get good agreement between the theoretical and observed amplitude ratios in all passbands, for the star HD 48501; and for this small value of f_T, the three observed modes are identified as $\ell = 1$ modes. They also showed that, with FC treatment it is impossible to get good agreement with observations, because the predicted values of f_T are too large.

In Fig. 8, we give the theoretical and observed Geneva photometric amplitude ratios we obtained for different TDC models of HD 48501. Error bars are given for the three observed components

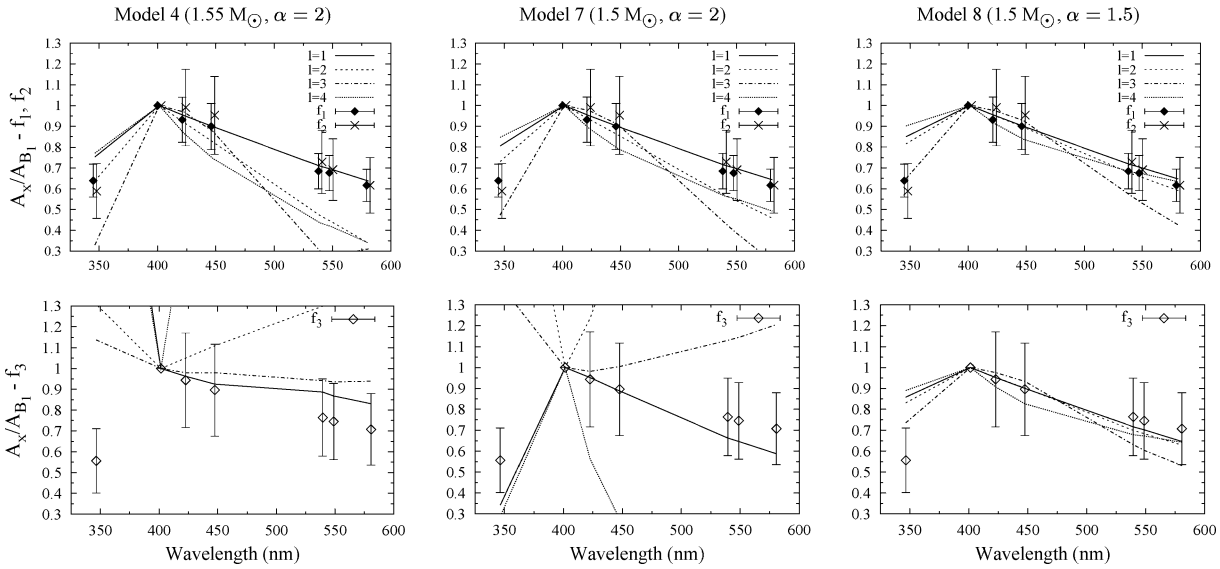

Figure 7. Geneva photometric amplitude ratios for different models of HD 12901. The top panels are for the f_1 and f_2 modes and the bottom panels are for the f_3 mode. The lines are the theoretical predictions for different ℓ values and the error bars represent the observations for the different frequencies. TDC treatment is adopted in all the models.

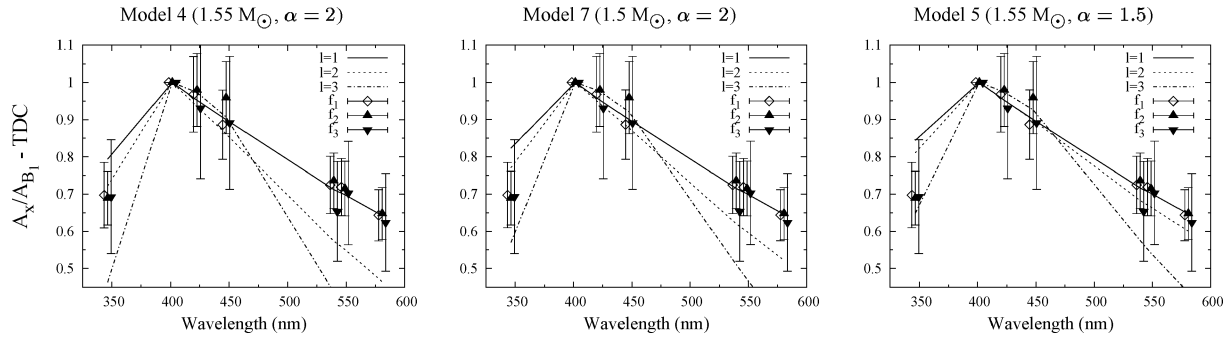

Figure 8. Geneva photometric amplitude ratios for different HD 48501 models. The lines are the theoretical predictions for different ℓ values and the error bars represent the observations for the three frequencies.

and the lines are the theoretical predictions for the frequency closest to component f_2 (theoretical results for the other components are very close). The left, middle and right panels give the results obtained for models 4, 7 and 5 of Table 1, respectively. We used MLT atmosphere models in all our computations. With TDC treatment, $\alpha = 2$ and $M = 1.55\,\mathrm{M}_\odot$ (left panel), f_T is the smallest and consequently, better agreement with observations can be obtained. However, f_T is not small enough to give good agreement for the critical U/B_1 amplitude ratio. We notice that the amplitude ratios of this best model in the other passbands indicate that the three observed components are $\ell = 1$ modes.

5 IMPORTANCE OF OBSERVATIONS IN THE ULTRAVIOLET

It was shown in the previous sections that, for too large values of f_T, amplitude ratios corresponding to $\ell = 1$, 2 and 4 are similar for passbands at the red side of the Balmer discontinuity ($\lambda > 364$ nm), but the amplitude ratios between two passbands at the blue and red side of the Balmer discontinuity (for example the Strömgren u/v ratio) disagree with observations for all these ℓ. In contrast, for small enough f_T values, it is possible to converge towards a unique solution in agreement with the observed amplitude ratios in all passbands. Observations in passbands bracketing the Balmer discontinuity is thus very important in γ Dor stars, giving better discrimination between different models and allowing better identification of ℓ. This can be explained as follows. We consider the case of an $\ell = 1$ mode, for which the geometrical term $(1 - \ell)(\ell + 2)\cos(\sigma t)$ in equation (1) is zero. The two remaining terms are the temperature term $f_\mathrm{T}\cos(\sigma t + \psi_T)(\alpha_{\mathrm{T}\lambda} + \beta_{\mathrm{T}\lambda})$ and the gravity term $-f_g\cos(\sigma t)(\alpha_{g\lambda} + \beta_{g\lambda})$. It is easily seen that, for large values of f_T, the temperature term dominates and $\delta m_{\lambda_1}/\delta m_{\lambda_2} \rightarrow b_{\ell\lambda_1}\alpha_{\mathrm{T}\lambda_1}/(b_{\ell\lambda_2}\alpha_{\mathrm{T}\lambda_2})$. In contrast, for small enough f_T the gravity term begins to play a non-negligible role compared to the temperature term and the amplitude ratios change with f_T. The Balmer drop is very sensitive to electronic pressure and thus to gravity. Hence, the values of $\alpha_{g\lambda}$ are very different in passbands below and above it, typically $\alpha_{gu} \simeq +0.07$, $\alpha_{gv} \simeq -0.04$ and $\alpha_{gy} \simeq -0.01$. The weight of the gravity term is thus larger in the u passband, hence the u/v amplitude ratio is more sensitive to f_T and comparison with observations enables us to constrain this parameter.

6 CONCLUSIONS

In this paper we have shown that, for γ Dor stars, the treatment of convection and the interaction between the convection and oscillations play a major role in the theoretical determination of the amplitude ratios between different photometric passbands and the phase lags between light and velocity curves. We have presented for the first time a significant improvement obtained by using TDC non-adiabatic models. This improvement makes the photometric mode identification in γ Dor stars possible. We have presented the application of our treatment to the mode identification and non-adiabatic seismic analysis of the stars γ Dor, 9 Aur, HD 207223, 12901 and 48501. A summary of our photometric identification of ℓ and the best α found for the four stars observed in multicolour photometry is given in Table 11. As a general conclusion of our study, we found that TDC models with $\alpha \simeq 2$ values corresponding to a thicker CE best agree with observations for γ Dor stars.

Table 11. Identification of ℓ and best α for the stars γ Dor, 9 Aur, HD 12901 and 48501.

Star	f_obs (c/d)	ℓ	f_obs (c/d)	ℓ	f_obs (c/d)	ℓ	α
γ Dor	1.32	1	1.36	1	1.47		2
9 Aur	0.79	2	0.77	2	0.34	1–2	2
HD 12901	1.22	1	1.40	1	2.19	1	2
HD 48501	1.09	1	1.29	1	1.20	1	2

For the star γ Dor, our photometric mode identification indicates that the components f_1 and f_2 are most probably $\ell = 1$ modes and best agreement is found for TDC models with $\alpha \simeq 2$. The same $\alpha \simeq 2$ value is required for mode excitation. For this value of α, the comparison between the theoretical and observed phase lags between light and velocity curves for the components f_2 and f_3 shows that TDC models agree better with the observations than do FC models.

For the star 9 Aur, our photometric mode identification indicates that the three observed components are most probably $\ell = 2$ modes and a better agreement is found for TDC models with $\alpha \simeq 2$. The same $\alpha \simeq 2$ value is required for the excitation of the modes; but even with this α, the mode with smallest frequency ($f_3 = 0.343$ c/d) is predicted to be stable. The comparison between the theoretical and observed phase lags between light and velocity curves for the components f_2 and f_3 shows that TDC models better agree with observations than FC models.

For the mono-periodic star HD 207223, the excitation of the observed mode is obtained for models with $\alpha \simeq 2$ and $\ell = 1$ mode. The comparison between the theoretical and the observed phase lags between light and velocity curves shows that TDC models agree much better with observations than do FC models.

For the star HD 12901, our photometric mode identification indicates that the three components are most probably $\ell = 1$ modes and a better agreement is found for TDC models with $\alpha \simeq 2$. However, the component with smallest period is predicted to be stable for an $\ell = 1$ mode; a higher degree ℓ is required to render this mode unstable.

For the star HD 48501, our photometric mode identification indicates that the three components are most probably $\ell = 1$ modes and the best agreement is found for TDC models with $\alpha \simeq 2$. The same $\alpha \simeq 2$ value is required for the modes excitation.

In this study, the main attention was given to the use of TDC models for the interpretation of the photometric amplitude ratios and phase differences in γ Dor stars and the identification of the degree ℓ of their pulsation modes. In the broader context of asteroseismology, the mode identification is a key step, but the final goal is to use all the information coming from the pulsation frequencies in order to improve the knowledge of the stellar interiors. Moya et al. (2005) proposed a method using the frequency ratios for the seismic modelling of γ Dor stars. Such analysis of the frequency content gives direct constraints on the Brunt-Väisälä frequency in the deep g-mode cavity; while our TDC non-adiabatic analysis constrains the characteristic of the superficial convective zone. Our future project is to combine these two methods to get information about both the deep interior and the superficial layers of γ Dor stars. A difficult problem in the seismic study of γ Dor stars is to determine the effect of rotation on the frequencies and on the energy of the oscillations. These effects will also be analysed in future studies.

ACKNOWLEDGMENTS

MAD acknowledges financial support by CNES. RG acknowledges financial support from the programme ESP2004-03855-C03-01. JDR acknowledges support from the Fund for Scientific Research–Flanders.

REFERENCES

Aerts C., Kaye A. B., 2001, ApJ, 553, 814
Aerts C., Krisciunas K., 1996, MNRAS, 278, 877
Aerts C., Cuypers J., De Cat P., Dupret M.-A., De Ridder J., Eyer L., Scuflaire R., Waelkens C., 2004, A&A, 415, 1079
Alexander D. R., Ferguson J. W., 1994, ApJ, 437, 879
Balona L. A., Stobie R. S., 1979, MNRAS, 189, 649
Balona L. A., Hearnshaw J. B., Koen C., Collier A., Machi I., Mkhosi M., Steenberg C., 1994a, MNRAS, 267, 103
Balona L. A., Krisciunas K., Cousins W. J., 1994b, MNRAS, 270, 905
Balona L. A., Böhm T., Foing B. H. et al., 1996, MNRAS, 281, 1315
Barban C., Goupil M. J., Van't Veer-Menneret C., Garrido R., Kupka F., Heiter U., 2003, A&A, 405, 1095
Canuto V. M., Goldman I., Mazzitelli I., 1996, ApJ, 473, 550
Christensen-Dalsgaard J., Däppen W., 1992, A&A, Rev., 4, 267
Claret A., 2000, A&A, 363, 1081
Dupret M.-A., 2002, PhD thesis, Bull. Soc. R. Sci. Liège, 5–6, 249
Dupret M.-A. et al., 2003a, Ap&SS, 284, 129
Dupret M.-A., De Ridder J., De Cat P., Aerts C., Scuflaire R., Noels A., Thoul A., 2003b, A&A, 398, 677
Dupret M.-A., Grigahcène A., Garrido R., Gabriel M., Scuflaire R., 2004, A&A, 414, L17
Dupret M.-A., Grigahcène A., Garrido R., Gabriel M., Scuflaire R., 2005, A&A, in press (Paper II)
Eyer L., Aerts C., 2000, A&A, 361, 201
Gabriel M., 1996, Bull. Astron. Soc. India, 24, 233
Garrido R., 2000, in Montgommery M., Breger M., eds, The 6th Vienna Workshop on δ Scuti and Related Stars. PASP Conf. Series, Vol. 210. Astron. Soc. Pac., San Francisco, p. 67
Grigahcène A., Dupret M.-A., Garrido R., Gabriel M., Scuflaire R., 2004, Comm. Asteroseismol., 145, 10
Grigahcène A., Dupret M.-A., Gabriel M., Garrido R., Scuflaire R., 2005, A&A, 434, 1055
Guzik J. A., Kaye A. B., Bradley P. A., Cox A. N., Neuforge C., 2000, ApJ, 542, L57
Handler G., 1999, IBVS, 4817, 1
Heiter U., Kupka F., van't Veer-Menneret C. et al., 2002, A&A, 392, 619
Iglesias C. A., Rogers F. J., 1996, ApJ, 464, 943
Kaye A. B., Handler G., Krisciunas K., Poretti E., Zerbi F. M., 1999a, PASP, 111, 840
Kaye A. B., Henry G. W., Fekel F. C., Hall D. S., 1999b, MNRAS, 308, 1081
Krisciunas K., Griffin R. F., Guinan E. F., Luedeke K. D., McCook G. P., 1995, MNRAS, 273, 662
Künzli M., North P., Kurucz R. L., Nicolet B., 1997, A&AS, 122, 51
Kurucz R. L., 1993, ATLAS9 Stellar Atmosphere Programs and 2 km s^{-1} grids. Kurucz CDROM No. 13
Kurucz R. L., 1998, http://kurucz.harvard.edu/grids.html
Mathias P., Le Contel J.-M., Chapellier E. et al., 2004, A&A, 417, 189
Moya A., Suarez J. C., Amado P. J., Martin-Ruiz S., Garrido R., 2005, A&A, 432, 189
Smalley B., 1993, A&A, 274, 391
Smalley B., Kupka F., 1997, A&A, 328, 349
Stamford P. A., Watson R. D., 1981, Ap&SS, 77, 131
Stütz C., Nendwich J., 2002, Vienna TempLogG v2 web interface: http://ams.astro.univie.ac.at/xtemplogg/main.php References for the calibrations in the manual at: http://ams.astro.univie.ac.at/templogg/Manual.php
Warner P. B., Kaye A. B., Guzik J. A., 2003, ApJ, 593, 1049
Watson R. D., 1988, Ap&SS, 140, 255
Zerbi F. M., Garrido R., Rodriguez E., Krisciunas K., Crowe R. A., Roberts M., 1997, MNRAS, 290, 401

This paper has been typeset from a TEX/LATEX file prepared by the author.